FFI RAPPORT

NUMERICAL SIMULATION OF LIGHT ARMOUR PIERCING AMMUNITION AGAINST CERAMICS

TELAND Jan Arild

FFI/RAPPORT-2005/00125

FFI-V/870/130

NUMERICAL SIMULATION OF LIGHT ARMOUR PIERCING AMMUNITION AGAINST CERAMICS

TELAND Jan Arild

FFI/RAPPORT-2005/00125

FORSVARETS FORSKNINGSINSTITUTT (FFI)
Norwegian Defence Research Establishment

P O BOX 25
N0-2027 KJELLER, NORWAY
REPORT DOCUMENTATION PAGE

1)	PUBL/REPORT NUMBER	2)	SECURITY CLASSIFICATION	3)	NUMBER OF PAGES
	FFI/RAPPORT-2005/00125		UNCLASSIFIED		27
1a)	PROJECT REFERENCE	2a)	DECLASSIFICATION/DOWNGRADING SCHEDULE		
	FFI-V/870/130		-		

4)	TITLE
	NUMERICAL SIMULATION OF LIGHT ARMOUR PIERCING AMMUNITION AGAINST CERAMICS

5)	NAMES OF AUTHOR(S) IN FULL (surname first)
	TELAND Jan Arild

6)	DISTRIBUTION STATEMENT
	Approved for public release. Distribution unlimited. (Offentlig tilgjengelig)

7) INDEXING TERMS

IN ENGLISH:		IN NORWEGIAN:	
a)	Simulation	a)	Simulering
b)	Ceramics	b)	Keramikk
c)	Penetration	c)	Penetration
d)		d)	
e)		e)	

THESAURUS REFERENCE:

8) ABSTRACT

Using the hydrocode Autodyn we perform numerical simulations of penetration into various combinations of ceramic armour and backing material. In particular we look at the penetration performance of two common 7.62 x 51 mm projectiles, namely the Bofors FFV and Fabrique Nationale P80. It is seen that the expected physical effects are reproduced in the numerical simulations and that, in principle, sensitivity studies can be performed using Autodyn to determine the optimal configuration of ceramic and backing material. However, lack of good material models may be a problem.

9)	DATE	AUTHORIZED BY	POSITION
		This page only	
	13. januar 2004	Bjarne Haugstad	Director of Research

CONTENTS

NUMERICAL SIMULATION OF LIGHT ARMOUR PIERCING AMMUNITION AGAINST CERAMICS

1   INTRODUCTION

In Project 870 one of the goals is to study penetration of various types of projectiles into (light) armour materials, especially ceramic armour. Such a system typically consists of one layer of ceramics followed by a backing layer, for example of aluminium. Various combinations of materials may give different results and it is difficult to tell in advance which combination of materials will work and what the optimal thicknesses of the materials are.

An advantage of numerical simulations is that it is very simple to perform sensitivity studies, varying the properties of the armour and seeing what happens. In this report we will examine the penetration of two particular common AP projectiles into different ceramic armour systems. This part is a purely numerical study since no experimental data was available for the configurations we will examine. The main purpose of the work was to become familiar with modelling penetration into ceramic armour systems and check that the expected physical effects can be reproduced using numerical simulations.

However, in addition, we also perform some simulations of other configurations where limited experimental data was available. Unfortunately, lack of material data for the experiments performed turn out to be a general problem.

2   CERAMIC ARMOUR SYSTEMS

It is desirable for an armour system to stop the required projectile while at the same time have as small mass as possible. Thus, the perfect armour system would have infinite strength and zero density. Unfortunately, no such materials exist, but ceramic materials may be considered nice substitute. They have some good properties since they are very hard despite having a low density. There is one drawback, though. Ceramic materials are brittle and can therefore easily break up, for example due to tensile waves generated from reflection at the rear end of the block. As a consequence, even if the ceramic material is able to stop the projectile itself, there could be severe scabbing effects. However, this problem can be fixed by putting a ductile backing material, f.ex. aluminium, behind the ceramic, whose task it will be to absorb the ceramic "rubble".

Figures 2.1-2.2 demonstrate the properties of ceramic armour very well. They are generated from numerical simulations using the hydrocode Autodyn. We will later look more in detail at how to model in such a situation, but currently we will only use these plots to underline some points about the workings of ceramic armour.

In Figure 2.1 we show the what happens on impact of a projectile onto a ceramic SiC plate. It is seen that there are several cracks and lots of spalling.
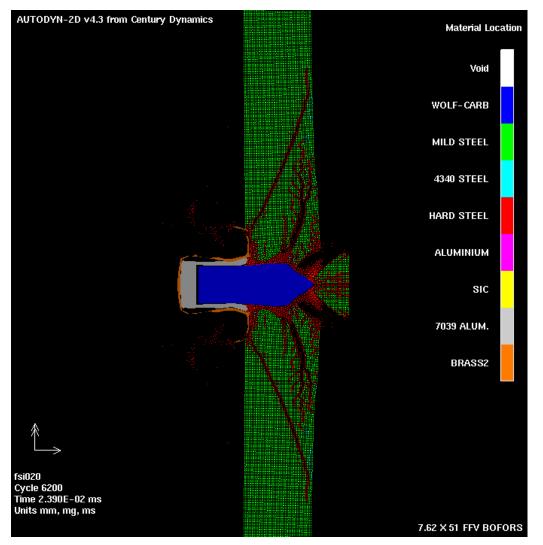

Figure 2.2: FFV projectile perforating a 10 mm SiC plate.

In Figure 2.2 we have the same situation except that the ceramic is backed up by an aluminium plate.
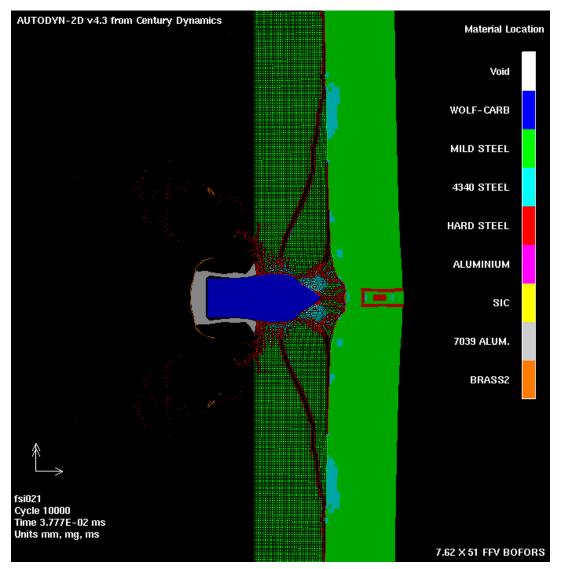
Figure 2.2: FFV projectile is stopped by a 10 mm SiC plate backed up by 10 mm Al5083.

In this case we see that the projectile does not even manage to penetrate the ceramic. There is some cracking and delamination. It is important to be aware that if the plates had been separated in space so that the projectile in effect went through two different penetration processes, then the projectile would have perforated both plates. However, when the plates are put together they easily stop the projectile.

The exact mechanisms of ceramic armour failure was first investigated by Wilkins et. al. (1) Using high-speed photography, flash x-ray and numerical models he postulated the following effects for small-caliber ammunition:

- The projectile tip is destroyed. This did not happen in Figure 2.2, but would have happened for a weaker projectile (ball).

- Fracture conoid is initated at the projectile-target interface. Spreads the load of the projectile onto a relatively wide area of the backing material. The fracture conoid is clearly seen in both Figure 2.1 and Figure 2.2.

- Backing plate yields at ceramic interface. This is also the case in the simulation, although Figure 2.2 illustrates the situation late on when the projectile has almost come to rest and the backing plate has returned to elasticity in most of the volume.

3   PROJECTILES

In this report we will especially study the 7.62 x 51 FFV Bofors AB projectile with a Wolfram-Carbide core and the 7.62 x 51 AP Fabrique National projectile with a hard steel core. The projectiles are shown in Figure 2.1.

7,62 AP NM 61
Prosjektilvekt : 9,71 g
Kjerne : Herdet stål
Vekt kjerne : 3,63 g

7,62 AP CG WC
Prosjektilvekt : 8,30 g
Kjerne : Wolfram karbid (?)
Vekt kjerne : 5,92 g

Figure 3.1: The projectiles and cores that are studied in this report.

We have so far been unable to dissect and examine the contents of the FN projectiles, but it is widely known (2) that NM61 projectiles from Raufoss, for which we have projectiles available, are made after (almost) the same standard. Further, 7.62 x 51 Carl Gustav (CG) with a tungsten carbide core are the same as 7.62 x 51 FFV from Bofors.

4   HYDROCODE MODEL

Numerical simulations were performed using the hydrocode Autodyn-2D (3). To use a 2D hydrocode, cylindrical symmetry has to be assumed. This means that crack patterns may not be correctly described. However, this is not very important for depth of penetration and ballistic limit, which were the results we were most interested in.

Autodyn has several different processors for modelling, including Lagrange, Euler and SPH. The Lagrange processor is typically suitable for objects that some strength and have an initial shape. The Euler processor is typically for a material with no pre-defined shape (like fluids, gases), but it is also often used for objects that will be strongly deformed (like a target in a penetration experiment). SPH is a meshless technique, often used for brittle objects to model cracks etc properly.

In our case the projectile core was expected to remain relatively intact, and it was therefore natural to model it using Lagrange. This made it very convenient to model the complete projectile using different Lagrangian subgrids.

4.1 Bofors FFV

The Bofors projectile was modelled using a total of seven Lagrangian subgrids (two for the core, two for the aluminium and three for the brass jacket. It is shown in Figure 3.1. The subgrids for the different materials were not joined together, but interacted with eachother using the interaction mechanism in Autodyn

Figure 4.1: 7.62 x 51 FFV Bofors projectile.

4.2 Fabrique National P80

The P80 projectile, shown in Figure 3.2 was modelled using a total of five Lagrangian subgrids (two for the core and three for the lead and brass part). The core was not joined to the outer parts, but interacted with the interaction option. The lead and brass was for simplicy put in the same subgrid.

Figure 4.2: 7.62 x 51 AP Fabrique National

4.3 Target

The target was to consist of one ceramic plate backed up by an Al5083 plate. Ceramics are brittle and the natural choice is therefore to use the SPH processor. This is also the

recommended method by Century Dynamics, producer of Autodyn (4). However, a disadvantage of using SPH it that the calculations take much longer so that computatio times can be become very long compared with Lagrange. To improve the situation we modelled only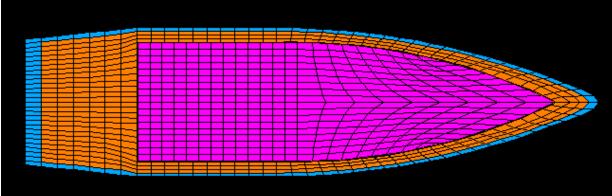 the central part of the target using SPH, but joined it to a Lagrange grid further out, where it was not expected to be very important to have the local effects (cracks etc.) absolutely correct. This speeded the simulations up considerably and sensitivity studies indicated no real difference in results (for penetration depth and ballistic limit) between this and a complete SPH ceramic plate.

The Al5083 is a ductile material and the obvious choice would then be either Lagrange or Euler grid. However, in order to be able to join the backing plate with the ceramic SPH-plate, we had to use Lagrange.

Thus, we used a joined SPH-Lagrange ceramic plate joined to a Lagrange Al5083-plate.

The aluminium was modelled completely in Lagrange. As an example, the set-up for one specific case is shown in Figure 4.3.

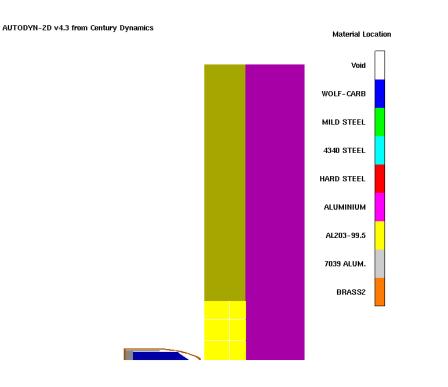*Figure 4.3: Impact onto 14 mm Al2O3 + 20 mm Al. The central part of the ceramic was modelled in SPH while the outer parts were modelled in Lagrange. The Aluminium was modelled completely in Lagrange.*

All target subgrids were joined together. This corresponds to a physical situation where the alumina is "glued" to the aluminium instead of just being put next to it (as would have been another alternative).

5   DUCTILE MATERIAL MODELS

To obtain realistic results, it is necessary that the material models used give a close description of actual materials. Since most of our simulations do not correspond to actual experiments that have been performed, it is difficult to know how accurate the results are.

5.1   Steel

We require a steel model both for the core of the 7.62 x 51 AP FN projectile. Steel is usually considered to be a simple material to obtain data for. In a hydrocode simulation, steel is usually described by elastic parameters and a yield strength. The yield strength depends can depend on various other variables, like plastic strain and the strain rate.

In Autodyn steel is often described using the Johnson-Cook model. The relationship between yield strength, plastic strain, strain rate and temperature is then given as follows:

$$Y = (A + B\varepsilon_p^n)(1 + C\ln\dot{\varepsilon}_p)(1 - T_H^m)$$

where A, B, C, n and m are parameters determining the material.

Unfortunately, for the steel core of the projectile, we only have available the Vicker's hardness number. On conversion to yield strength, using standard conversion tables, we obtained a yield stress of around 2.35 GPa. This is a very high value and various references (5) indicate that such a hard steel might not even exist. For more details, see (6) for a more detailed discussion on conversion from Vicker's hardness to yield strength.

Further, it is then clear that only an estimate for the value of A is obtained from the Vicker's Hardness test. No data is available for B,C, n or m, which describe the strain hardening and strain rate sensitivity of the material. In order to get estimates for these parameters, we have used the same parameters as for the 4340 steel model in the Autodyn material library. It is clear that this is a very crude approximation, assuming implicitly that all steel types have the same strain hardening and strain rate dependence. Further, this assumption might be especially inaccurate for materials that have already been "pre-hardened" like the core of the FN projectile (the physics is unknown to us at the moment).

The other steel parameters have not been changed, which means that the elastic moduli and the strain rate dependence is similar for all the steel models.   However, this should not be too important since elastic parameters have very little influence on the penetration process.

5.2   Lead

For the lead jacket of the projectile we used a material model based on the lead model in the Autodyn material library. It uses the shock equation of state. In addition we added a yield limit from (7) and a numerical erosion criterion of 2.5.

5.3   Brass

For the brass we used a material model based on the brass model in the Autodyn material library. It uses the shock equation of state. In addition we added a yield limit from (7) and a numerical erosion criterion of 2.5.

5.4   AA5083-H116

The aluminium AA5083-H116 material mode, which is used in the backing plates was obtained from Børvik et.al (8). It consists of a Johnson-Cook yield model as well as numerical erosion.

6   CERAMIC MATERIAL MODELS

Ceramic materials are harder to describe than ductile materials. Often the Johnson-Holmquist model (9) has been used and we therefore describe it in relative detail.

6.1   Johnson-Holmquist material model

The Johnson-Holmquist (strength/damage) model is commonly used to describe ceramic materials. Several sources (10) have reported that it provides good results while capturing the most important physical effects of ceramic response to ballistic impact. However, it must be remembered that it is not really derived from fundamental physics and it relies on several empirical parameters that are difficult to determine in a material test. Further, there are some signs that it will not always give good results (11,12). Nevertheless, in the following, we briefly describe the Johnson-Holmquist model.

Actually there are two Johnson-Holmquist models, referred to as JH-1 (13) and JH-2 (9). The first version had some shortcomings which were adressed in the JH-2 model, which therefore is the most commonly used. The JH-2 model introduces a parameter called damage to account for damage to the material. The main idea is that when damage increases, the yield limit (amongst other variables) of the material decreases so that a damaged material will yield more easily. In a hydrocode simulation, each cell, can then obtain a different yield limit depending on how much damage it has sustained.

The damage variable is one way to macroscopically account for several effects on the microlevel. This is clearly an approximation, but it may nonetheless be quite accurate. The variable takes a value between 0 and 1, where 0 corresponds to an undamaged material and 1 to a completely damaged material. Having introduced the damage variable, there are basically two questions which must be answered:

- How to define damage in terms of other macroscopic parameters?

- How to relate the yield limit to the damage?

In the JH-2 model, the second question is answered in the following way:

$$Y = (1-D)Y_i + DY_f$$

where the index i means intact material and f means completely failed material. We see that for an undamaged material $(D=0), Y = Y_i$, whereas a completely failed material $(D=1)$ has $Y = Y_f$ with the yield limit being a linear interpolation for D between zero and one. Thus, it will be necessary to supply two yield limits for a material described by the Johnson-Holmquist model.

The first question has a little more complicated answer. The damage parameter itself is defined in terms plastic strain. It starts at zero and is then incremented according to the following formula each time the plastic strain is increased in an element:

$$\Delta D = \frac{\Delta \varepsilon_p}{D_1 (P+T)^{D_2}}$$

Thus, how much the damage increases is incremented depends on the two (empirical?) parameters D1 and D2, which must be supplied to the model. Their value will of course depend on which materials we are trying to describe.

A big problem is that the coefficients D1 and D2 are difficult (or impossible?) to measure in a simple material test. The normal approach is to calibrate the constants to penetration experiments. FFI has not yet performed any experiments and therefore has to rely on values published in different literature.

6.2   Tungsten carbide

The Tungsten-Carbide model for the 7.62 x 51 FFV Bofors projectile core was obtained from (11). It uses a linear EOS together with a Mohr-Coulomb yield model and a user-defined failure model. The failure model was implemented as a user subroutine in Autodyn.

6.3   Alumina

We performed simulations both with alumina 99.5% and Silisium Carbide backed by aluminium armour. The material model for alumina 99.5% was found in the Autodyn material library, where the Johnson-Holmquist damage model was used. However, it should be noted that the parameters for this material models differs from the one given in (14).

6.4   Silisium Carbide

The Silisium Carbide model was found in (14). The Johnson-Holmquist damage model was used.

7   IMPACT AGAINST ALUMINA AND ALUMINIUM TARGET

Having obtained material models for the materials of interest, we then performed simulations of a projectile impacting a target configuration of a ceramic backed up by a ductile material.

At the moment of writing, no good experimental data was available for us to compare with, so the simulations were mainly intended to give an insight into what could be achieved using numerical simulations. In our simulations we have used the Bofors 7.62 x 51 FFV with an estimated impact velocity of 900 m/s (15).

In the first case, we performed simulations varying the thickness of the alumina and aluminium, trying to find the necessary amount of alumina required to stop a projectile for a given aluminium backing. In practise, we looked at backings of 10 mm, 15.2 mm, 20 mm, 28 mm and 38 mm. We then ran several simulations for these backings varying the alumina thickness until we just managed to stop the projectile.

The plates were cylindrical (so we could use Autodyn-2D) and had a diameter of 200 mm. Because of the relative small thickness of the target we could be reasonably sure that boundary effects would not be important with such a set-up.

The alumina was modelled using two subgrids: one in SPH and the other in Lagrange. SPH is the recommended processor for ceramics (4)], but it is quite much slower than the Lagrange processor. As a compromise, the zone around the projectile was modelled in SPH while the zone further out was modelled using a Lagrange subgrid.

The results for the ballistic limits are given in Table 7.1.

Table 7.1: Combinations of Al2O3 and Al5083 that stop a 7.62 x 51 mm FN projectile.

Al2O3 thickness	Al5083 thickn.	Total thickness	Total mass/area	Total cost/area
0	47	47	125.02	
4.8	38	42.8	119.75	
11.5	28	39.5	119.21	
17	20	37	119.33	
22	15.2	37.2	126.01	
26	10	36	127.74	

We see that as expected the total thickness required to stop the projectile becomes smaller when we use thicker alumina. However, since alumina is heavier than aluminium, the total mass does not change much. It may look like there is a minimum mass somewhere around 12 mm Al2O3, but the differences are very small. With all the uncertainties surrounding the material models, it would not make sense to perform further simulations in order to locate this point of minimum requiredmass.

8   IMPACT AGAINST SILICON-CARBIDE AND ALUMINIUM TARGET

For comparison we also performed simulations with another ceramic, Silicon-Carbide instead of alumina 99.5%. The backing was still Aluminium 5083. The material model for SiC was taken from (14).

We looked at aluminium thicknesses of 4, 18, 28 38 and 47 mm and varied the SiC thickness to find the minimum requirement to just be able to stop the projectile.

Again the ceramic subgrid was part SPH and Lagrange, joined to the Aluminium backing. The plate diameter was 200 mm. The results are given in Table 8.1.

Table 8.1: Combinations of Sic and Al5083 that stop a 7.62 x 51 mm FN projectile.

SiC thickness	Al5083 thickn.	Total thickness	Total mass/area	Total cost/area
0	47	47	125.02	
2	38	40	107.4	
4.4	28	32.4	88.4	
6.5	18	24.5	68.4	
10.7	4	14.7	44.5	

Here we see a clear tendency that more ceramic gives the lowest mass for protection, unlike for alumina where the decreased thickness was compensated for by the alumina having larger density and therefore larger total mass. For SiC it is clearly an advantage to use as much ceramic as possible, given that total mass is the most important parameter. Unfortunately, if cost is also taken into account, SiC is more expensive than alumina and a protection with only SiC may therefore be considerably more expensive. [[Hazell sier at forskjellen i pris er en faktor 5, mens utregninger fra Bryn James gir en større faktor]]

9   OTHER MATERIALS (COMPARISON WITH DATA)

In this chapter we compare simulation results with some available data. In Janes (16) there is an overview of data for armour thicknesses required to stop a 7.62 x 51 mm AP projectile. It is not stated explicitly which projectile the data is for, so we will perform simulations both for the Bofors FN projectile with tungsten carbide core (900 m/s) and the P80 projectile with a steel core (820 m/s).

In (16) there is data for the armour required to stop a projectile. We performed simulations for exactly these thicknesses and saw what happened.

9.1   Al5083

The required thickness is said to be 48 mm. Simulations give that the FFV projectile stops for 48 mm and just comes through for 46.8 mm, so this is excellent agreement

For the P80 projectile the required thickness is about 45 mm, also in good agreement. (44 mm Al5083 gives an exit velocity of 158 m/s).

9.2   Alumina + backing

According to (16), 6 mm A12O3 + 11 mm Al5083 will stop the projectile. However, for the FFV projectile, the simulations give an exit velocity 651 m/s in this case. In fact, as we saw in

Chapter 7, nearly 30 mm Al5803 is required if we have only 6 mm Al2O3. For the P80 projectile we get an exit velocity of 635 m/s, so agreement is very poor for both projectiles in this case.

Further, in (16) it is said that 6.4 mm Al2O3 + 5.6 mm HHS (High Hardness steel) will stop the projectiles. No information was given about the hardness or yield strength of the HHS, so in our simulations we used the same HHS model as in (6).

For the P80 projectile we got perforation at an exit velocity of 393 m/s, which is not in that bad agreement with the experiments, as a increasing the steel thickness by 1-2 mm would probably stop perforation. However, for the FFV projectile, agreement was still very bad with an exit velocity of 623 m/s.

In total, agreement was quite disappointing for this configuration. However, it should be remembered that we had no information about which projectile were used and what the material model was for both the projectiles and the targets.

9.3   Titanium alloy

The article in (16) also claims that 20 mm of the titanium alloy Ti-6Al-4V will stop the projectile. The simulations also give 20 mm for the FFV projectile, so this time the agreement is excellent.

For the P80 projectile we find that around 17 mm is enough to stop the projectile, which is also a reasonable agreement.

Thus, it appears that agreement is very good for a single material target but not so good for a multilayer target. However, since we are not aware of details of the experiments that have been performed to arrive at these results, we should be careful in drawing any quick conclusions.

10   SUMMARY

We have looked at penetration simulations for two particular 7.62 x 51 mm projectiles, FFV and P80. Data is limited but we performed a parametric study to see how much ceramic armour and backing would be needed to stop each of these projectiles, for two different ceramics. Further, we performed some simulations and compared with (vague) experimental data from Janes. For some cases agreement was very good, but it seemed that ceramic + backing would provide more protection in reality than in the simulation. However, due to the lack of proper data of the circumstances of the experiment, we should be careful in drawing any certain conclusions at such an early stage.

The physical effects seemed to be predicted qualitatively correct by the hydrocode. It was seen that backing would have to be close to the ceramic, preferably attached, to have full effect.

Thus, it should be possible to use Autodyn to simulate more complex armoured target configurations.

References

(1)   Wilkins M, Cline C, The importance of material properties in ceramic armor, Proceedings of the Ceramic Armor Technology Symposium (USA), 13-18, January 1969

(2)   Fykse H, Private conversation

(3)   Autodyn Theory Manual, Century Dynamics Ltd.

(4)   Robertson, Ian (Century Dynamics), Private e-mail

(5)   Dullum O, Fykse H, Private conversation

(6)   Teland J A, Numerical simulations of light armour piercing ammunition against steel, FFI/RAPPORT-2005/00126

(7)   Børvik T, Langseth M, Jenssen A, Langberg H, Smedsrød Ø, Use of aluminium panels as lightweight ballistic protection, Proceedings of the Norway-Singapore Workshop on Protection, Oslo, 3-5 november 2003

(8)   Børvik T, Clausen A H, Hopperstad, O S, Langseth M, Perforation of AA5083-H116 alumium plates with conical-nose steel projectiles – experimental study,Int J Impact Engng Volume 30, Issue 4, pp. 367-384, 2004

(9)   Johnson G R, Holmquist T J, An improved computational constitutive model for brittle materials, High pressure science and technology 1994, American Institute of Physics

(10)   Kaufmann C, Cronin D S, Worswick M J, Bourget D, Numerical modelling of the ballistic response of ceramic tiles supported by semi-infinite metallic backings, Personal Armour Systems Symposium - PASS, The Hague, The Netherlands, November 18-22, 2002

(11)   Moxnes J F, Private conversation

(12)   Galvez F, Cendon D, Sanches-Galvez V, Experimental and numerical comparison of failure of ceramic tiles impacted by FSP's, Proceedings of the 21st Int Symposium on Ballistics, Adelaide, Australia, 19-23 April 2004

(13)   Johnson G R, Holmquist T J, A computational constitutive model for brittle materials subjected to large strains, Shock-wave and High strain-rate phenomena in materials, New York, 1075-1081, 1992

(14)   Cronin D S, Bui K, Kaufmann C, McIntosh G, Berstad T, Implemenation and validation of the Johnson-Holmquist Ceramic Material model in LS-Dyna, Proceedings of the 4th European LS-Dyna Users Conference

(15)   Fykse H, Private e-mail

(16)   Ogorkiewicz R M, Armor for Light Combat Vehicles, Janes International Defense Review, 41-45, 2002

A MATERIAL MODELS

MATERIAL NAME: WOLF-CARB

EQUATION OF STATE: Compaction

Reference density (g/cm3) : 1.45500E+01
Density #1 (Pressure) (g/cm3) : 1.45500E+01
Density #2 (Pressure) (g/cm3) : 1.70000E+01
Density #3 (Pressure) (g/cm3) : 0.00000E+00
Density #4 (Pressure) (g/cm3) : 0.00000E+00
Density #5 (Pressure) (g/cm3) : 0.00000E+00
Density #6 (Pressure) (g/cm3) : 0.00000E+00
Density #7 (Pressure) (g/cm3) : 0.00000E+00
Density #8 (Pressure) (g/cm3) : 0.00000E+00
Density #9 (Pressure) (g/cm3) : 0.00000E+00
Density #10 (Pressure) (g/cm3) : 0.00000E+00
          Pressure #1 (kPa)   : 0.00000E+00
          Pressure #2 (kPa)   : 5.81000E+07
          Pressure #3 (kPa)   : 0.00000E+00
          Pressure #4 (kPa)   : 0.00000E+00
          Pressure #5 (kPa)   : 0.00000E+00
          Pressure #6 (kPa)   : 0.00000E+00
          Pressure #7 (kPa)   : 0.00000E+00
          Pressure #8 (kPa)   : 0.00000E+00
          Pressure #9 (kPa)   : 0.00000E+00
          Pressure #10 (kPa)   : 0.00000E+00
Density #1 (Soundspeed) (g/cm3) : 1.45500E+01
Density #2 (Soundspeed) (g/cm3) : 1.70000E+01
Density #3 (Soundspeed) (g/cm3) : 0.00000E+00
Density #4 (Soundspeed) (g/cm3) : 0.00000E+00
Density #5 (Soundspeed) (g/cm3) : 0.00000E+00
Density #6 (Soundspeed) (g/cm3) : 0.00000E+00
Density #7 (Soundspeed) (g/cm3) : 0.00000E+00
Density #8 (Soundspeed) (g/cm3) : 0.00000E+00
Density #9 (Soundspeed) (g/cm3) : 0.00000E+00
Density #10 (Soundspeed) (g/cm3) : 0.00000E+00
          Soundspeed #1 (m/s)   : 4.86900E+03
          Soundspeed #2 (m/s)   : 4.50500E+03
          Soundspeed #3 (m/s)   : 0.00000E+00
          Soundspeed #4 (m/s)   : 0.00000E+00
          Soundspeed #5 (m/s)   : 0.00000E+00
          Soundspeed #6 (m/s)   : 0.00000E+00

Soundspeed #7 (m/s)   : 0.00000E+00
Soundspeed #8 (m/s)   : 0.00000E+00
Soundspeed #9 (m/s)   : 0.00000E+00
Soundspeed #10 (m/s)   : 0.00000E+00

STRENGTH MODEL: M-O Granular

Pressure #1 (kPa)   : -3.00000E+06
Pressure #2 (kPa)   : -9.00000E+05
Pressure #3 (kPa)   : 1.80000E+06
Pressure #4 (kPa)   : 4.98000E+07
Pressure #5 (kPa)   : 0.00000E+00
Pressure #6 (kPa)   : 0.00000E+00
Pressure #7 (kPa)   : 0.00000E+00
Pressure #8 (kPa)   : 0.00000E+00
Pressure #9 (kPa)   : 0.00000E+00
Pressure #10 (kPa)   : 0.00000E+00
Yield Stress #1 (kPa)   : 0.00000E+00
Yield Stress #2 (kPa)   : 2.75000E+06
Yield Stress #3 (kPa)   : 5.50000E+06
Yield Stress #4 (kPa)   : 6.15000E+07
Yield Stress #5 (kPa)   : 0.00000E+00
Yield Stress #6 (kPa)   : 0.00000E+00
Yield Stress #7 (kPa)   : 0.00000E+00
Yield Stress #8 (kPa)   : 0.00000E+00
Yield Stress #9 (kPa)   : 0.00000E+00
Yield Stress #10 (kPa)   : 0.00000E+00
Density #1 (Yield Stress) (g/cm3) : 1.30000E+01
Density #2 (Yield Stress) (g/cm3) : 1.50000E+01
Density #3 (Yield Stress) (g/cm3) : 1.60000E+01
Density #4 (Yield Stress) (g/cm3) : 1.70000E+01
Density #5 (Yield Stress) (g/cm3) : 1.80000E+01
Density #6 (Yield Stress) (g/cm3) : 1.90000E+01
Density #7 (Yield Stress) (g/cm3) : 2.00000E+01
Density #8 (Yield Stress) (g/cm3) : 2.10000E+01
Density #9 (Yield Stress) (g/cm3) : 2.20000E+01
Density #10 (Yield Stress) (g/cm3) : 2.30000E+01
Yield Stress #1 (kPa)   : 3.66700E+06
Yield Stress #2 (kPa)   : 3.66700E+06
Yield Stress #3 (kPa)   : 3.66700E+06
Yield Stress #4 (kPa)   : 3.66700E+06
Yield Stress #5 (kPa)   : 3.66700E+06
Yield Stress #6 (kPa)   : 3.66700E+06
Yield Stress #7 (kPa)   : 3.66700E+06
Yield Stress #8 (kPa)   : 3.66700E+06

Yield Stress #9 (kPa) : 3.66700E+06
Yield Stress #10 (kPa) : 3.66700E+06
Density #1 (Shear Modulus) (g/cm3) : 1.30000E+01
Density #2 (Shear Modulus) (g/cm3) : 1.50000E+01
Density #3 (Shear Modulus) (g/cm3) : 1.60000E+01
Density #4 (Shear Modulus) (g/cm3) : 1.70000E+01
Density #5 (Shear Modulus) (g/cm3) : 1.80000E+01
Density #6 (Shear Modulus) (g/cm3) : 1.90000E+01
Density #7 (Shear Modulus) (g/cm3) : 2.00000E+01
Density #8 (Shear Modulus) (g/cm3) : 2.10000E+01
Density #9 (Shear Modulus) (g/cm3) : 2.20000E+01
Density #10 (Shear Modulus) (g/cm3) : 2.30000E+01
Shear Modulus #1 (kPa) : 1.52900E+08
Shear Modulus #2 (kPa) : 1.52900E+08
Shear Modulus #3 (kPa) : 1.52900E+08
Shear Modulus #4 (kPa) : 1.52900E+08
Shear Modulus #5 (kPa) : 1.52900E+08
Shear Modulus #6 (kPa) : 1.52900E+08
Shear Modulus #7 (kPa) : 1.52900E+08
Shear Modulus #8 (kPa) : 1.52900E+08
Shear Modulus #9 (kPa) : 1.52900E+08
Shear Modulus #10 (kPa) : 1.52900E+08

FAILURE MODEL: User

Parameter FC(3)   : 3.00000E+00
Parameter FC(4)   : 1.00000E+01
Parameter FC(5)   : 1.00000E+04
Parameter FC(6)   : 1.00000E+00
Parameter FC(7)   : 9.00000E-01
Parameter FC(8)   : 1.01000E+20
Parameter FC(9)   : 1.01000E+20
Parameter FC(10)   : 1.01000E+20
Parameter FC(11)   : 1.01000E+20
Parameter FC(12)   : 1.01000E+20
Parameter FC(13)   : 1.01000E+20
Parameter FC(14)   : 1.01000E+20
Parameter FC(15)   : 1.01000E+20
Parameter FC(16)   : 1.01000E+20
Parameter FC(17)   : 1.01000E+20
Parameter FC(18)   : 1.01000E+20
Parameter FC(19)   : 1.01000E+20
Parameter FC(20)   : 1.01000E+20
Parameter FC(21)   : 1.01000E+20
Parameter FC(22)   : 1.01000E+20

Parameter FC(23)   : 1.01000E+20
Parameter FC(24)   : 1.01000E+20
Parameter FC(25)   : 1.01000E+20
Parameter FC(26)   : 1.01000E+20
Parameter FC(27)   : 1.01000E+20
Parameter FC(28)   : 1.01000E+20
Parameter FC(29)   : 1.01000E+20
Parameter FC(30)   : 1.01000E+20
Parameter FC(31)   : 1.01000E+20
Parameter FC(32)   : 1.01000E+20
Parameter FC(33)   : 1.01000E+20
Parameter FC(34)   : 1.01000E+20
Parameter FC(35)   : 1.01000E+20
Parameter FC(36)   : 1.01000E+20
Parameter FC(37)   : 1.01000E+20
Parameter FC(38)   : 1.01000E+20
Parameter FC(39)   : 1.01000E+20
Parameter FC(40)   : 1.01000E+20
Parameter FC(25)   : 1.01000E+20
Parameter FC(26)   : 1.01000E+20

EROSION MODEL: None

MATERIAL NAME: 4340 STEEL

EQUATION OF STATE: Linear

Reference density (g/cm3) : 7.83000E+00
Bulk Modulus (kPa)   : 1.59000E+08
Reference Temperature (K)   : 3.00000E+02
Specific Heat (C.V.) (J/kgK) : 4.77000E+02

STRENGTH MODEL: Johnson-Cook

Shear Modulus (kPa)   : 8.18000E+07
Yield Stress (kPa)   : 7.92000E+05
Hardening Constant (kPa)   : 5.10000E+05
Hardening Exponent   : 2.60000E-01
Strain Rate Constant   : 1.40000E-02
Thermal Softening Exponent   : 1.03000E+00
Melting Temperature (K)   : 1.79300E+03

FAILURE MODEL: None

EROSION MODEL: None

MATERIAL NAME: MILD STEEL

EQUATION OF STATE: Linear

Reference density (g/cm3) : 7.83000E+00
Bulk Modulus (kPa)   : 1.59000E+08
Reference Temperature (K)   : 3.00000E+02
Specific Heat (C.V.) (J/kgK) : 4.77000E+02

STRENGTH MODEL: Johnson-Cook

Shear Modulus (kPa) : 8.18000E+07
Yield Stress (kPa) : 2.90000E+05
Hardening Constant (kPa) : 5.10000E+05
Hardening Exponent   : 2.60000E-01
Strain Rate Constant   : 1.40000E-02
Thermal Softening Exponent   : 1.03000E+00
Melting Temperature (K) : 1.79300E+03

FAILURE MODEL: None

EROSION MODEL: Inst. Geo. Strain

Erosion Strain   : 4.00000E+00

MATERIAL NAME: HARD STEEL

EQUATION OF STATE: Linear

Reference density (g/cm3) : 7.83000E+00
Bulk Modulus (kPa)   : 1.59000E+08
Reference Temperature (K)   : 3.00000E+02
Specific Heat (C.V.) (J/kgK) : 4.77000E+02

STRENGTH MODEL: Johnson-Cook

Shear Modulus (kPa)   : 8.18000E+07
Yield Stress (kPa)   : 1.14300E+06
Hardening Constant (kPa)   : 5.10000E+05
Hardening Exponent   : 2.60000E-01
Strain Rate Constant   : 1.40000E-02
Thermal Softening Exponent   : 1.03000E+00
Melting Temperature (K)   : 1.79300E+03

FAILURE MODEL: None

EROSION MODEL: Inst. Geo. Strain

Erosion Strain   : 4.00000E+00

MATERIAL NAME: BRASS2

EQUATION OF STATE: Shock

Reference density (g/cm3) : 8.45000E+00
Gruneisen coefficient   : 2.04000E+00
Parameter C1 (m/s)   : 3.72600E+03
Parameter S1   : 1.43400E+00
Parameter Quad. S2 (s/m)   : 0.00000E+00
Relative volume, VE   : 0.00000E+00
Relative volume, VB   : 0.00000E+00
Parameter C2 (m/s)   : 0.00000E+00
Parameter S2   : 0.00000E+00
Reference Temperature (K)   : 0.00000E+00
Specific Heat (C.V.) (J/kgK) : 0.00000E+00

STRENGTH MODEL: Vonmises

Shear Modulus (kPa)   : 3.00000E+07
Yield Stress (kPa)   : 6.90000E+04

FAILURE MODEL: None

EROSION MODEL: Inst. Geo. Strain

Erosion Strain   : 2.00000E+00

MATERIAL NAME: 7039 ALUM.

EQUATION OF STATE: Shock

Reference density (g/cm3) : 2.77000E+00
Gruneisen coefficient   : 2.00000E+00
     Parameter C1 (m/s)   : 5.32800E+03
     Parameter S1   : 1.33800E+00
  Parameter Quad. S2 (s/m)   : 0.00000E+00
  Relative volume, VE   : 0.00000E+00
  Relative volume, VB   : 0.00000E+00
     Parameter C2 (m/s)   : 0.00000E+00
     Parameter S2   : 0.00000E+00
Reference Temperature (K)   : 3.00000E+02
Specific Heat (C.V.) (J/kgK) : 8.75000E+02

STRENGTH MODEL: Johnson-Cook

   Shear Modulus (kPa)   : 2.76000E+07
     Yield Stress (kPa)   : 3.37000E+05
  Hardening Constant (kPa)   : 3.43000E+05
   Hardening Exponent   : 4.10000E-01
  Strain Rate Constant   : 1.00000E-02
Thermal Softening Exponent   : 1.00000E+00
   Melting Temperature (K)   : 8.77000E+02

FAILURE MODEL: None

EROSION MODEL: None

MATERIAL NAME: ALUMINIUM

EQUATION OF STATE: Linear

Reference density (g/cm3) : 2.66000E+00
Bulk Modulus (kPa)   : 6.86200E+07
Reference Temperature (K)   : 0.00000E+00
Specific Heat (C.V.) (J/kgK) : 0.00000E+00

STRENGTH MODEL: Johnson-Cook

Shear Modulus (kPa)   : 2.63320E+07
Yield Stress (kPa)   : 1.67000E+05
Hardening Constant (kPa)   : 5.96000E+05
Hardening Exponent   : 5.51000E-01
Strain Rate Constant   : 1.00000E-03
Thermal Softening Exponent   : 8.59000E-01
Melting Temperature (K)   : 8.93000E+02

FAILURE MODEL: Hydro

Hydro Tensile limit (PMIN) (kPa)   : -2.75000E+05
Reheal   : Yes
Crack Softening, Gf (J/m2) : 0.00000E+00
or, Kc2 (mN2/mm3): 0.00000E+00

EROSION MODEL: Inst. Geo. Strain

Erosion Strain   : 4.00000E+00